Wrht: Efficient All-reduce for Distributed DNN Training in Optical Interconnect Systems

Fei Dai*, Yawen Chen, Zhiyi Huang, Haibo Zhang
University of Otago, Dunedin, New Zealand
travis@cs.otago.ac.nz

ABSTRACT

Communication efficiency is crucial for accelerating distributed deep neural network (DNN) training. All-reduce, a vital communication primitive, is responsible for reducing model parameters in distributed DNN training. However, most existing All-reduce algorithms, designed for traditional electrical interconnect systems, fall short due to bandwidth limitations. Optical interconnects, with superior bandwidth, low transmission delay, and less power consumption, emerge as viable alternatives. We propose Wrht (Wavelength Reused Hierarchical Tree), an efficient scheme for implementing the All-reduce operation in optical interconnect systems. Wrht leverages wavelength-division multiplexing (WDM) to minimize the communication time in distributed data-parallel DNN training. We calculate the required wavelengths, minimum communication steps, and optimal communication time, considering optical communication constraints. Simulations with real-world DNN models indicate that Wrht notably reduces communication time. On average, compared with three conventional All-reduce algorithms, Wrht achieves reductions of 65.23%, 43.81%, and 82.22% respectively in optical interconnect systems, and 61.23% and 55.51% compared with two algorithms in electrical systems. This highlights Wrht's potential to enhance communication efficiency in DNN training using optical interconnects.

CCS CONCEPTS

• **Computing methodologies → Parallel algorithms**; **Distributed artificial intelligence**.

KEYWORDS

Optical interconnects, All-reduce, distributed training, DNN, WDM

ACM Reference Format:
Fei Dai*, Yawen Chen, Zhiyi Huang, Haibo Zhang. 2023. Wrht: Efficient All-reduce for Distributed DNN Training in Optical Interconnect Systems. In *52nd International Conference on Parallel Processing (ICPP 2023), August 07–10, 2023, Salt Lake City, UT, USA*. ACM, New York, NY, USA, 10 pages. https://doi.org/10.1145/3605573.3605624

ICPP 2023, August 07–10, 2023, Salt Lake City, UT, USA

ACM ISBN 979-8-4007-0843-5/23/08…$15.00
https://doi.org/10.1145/3605573.3605624

1 INTRODUCTION

Deep neural networks (DNNs) find extensive applications in fields like computer vision, natural language processing, and robotics [16]. To accelerate the training of large-scale DNNs, such as Bert, the task is distributed among several workers, enhancing model convergence with parallel training. Data parallelism is a prevalent approach in which each worker uses its local dataset for DNN training and iteratively shares model parameters (e.g., gradients) with others. Stochastic gradient descent (SGD), a common DNN training method, frequently calls for data communications for All-reduce operations in distributed deep learning (DL) [7]. The goal of the All-reduce operation is to ensure that every worker receives the model parameters from all other workers and subsequently applies the reduction operation to obtain the averaged model parameters. It has been shown that the communications for All-reduce with a large number of workers may occupy 50-90% of per-iteration training time in current traditional electrical networks [35]. Therefore, creating scalable and efficient All-reduce algorithms is crucial to cut down communication time in distributed DNN training.

The communication time in traditional electrical interconnect systems can be excessively long due to the limited bandwidth of electrical routers, high network latency, and congestion [24]. This can lead to degraded training performance when the communication overhead outweighs the benefits of parallel computation. However, the emergence of CMOS-compatible optical devices [34] is opening up the possibility of using optical intra/inter-chip network connections, which offer high bandwidth, reduced transmission delay, and lower power consumption. Furthermore, optical interconnects can use different wavelengths in a waveguide, facilitated by wavelength-division multiplexing (WDM), to enable parallel data transmission. Several architectures using optical interconnect such as RAMP [20], TeraRack [10] and Hipoλaos [27], designed for distributed DNN training, are now available. These can potentially be employed to efficiently implement All-reduce operations.

However, most existing All-reduce algorithms are not designed for optical interconnects. They are designed for electrical interconnect systems and do not take advantage of the optical features such as parallel data transmission with WDM. For instance, the well-known Ring All-reduce algorithm takes $2(n-1)$ steps to finish the All-reduce communications [4], where n is the number of workers. However, such method is not suitable for optical interconnect system because it only assumes one wavelength for transmission in each step, failing to take advantage of WDM of optical interconnect. Therefore, it is necessary to design an efficient All-reduce algorithm for optical interconnect in order to utilize WDM for parallel data transmission and reduce the communication time of the All-reduce operation.

In this paper, we propose an efficient All-reduce scheme named WRHT in an optical ring interconnect system with the objective of minimizing the number of communication steps and communication time for All-reduce operation. We use ring topology for the system because it is a popular topology used in existing optical prototypes such TeraRack [10]. The core concept of WRHT is to implement the All-reduce operation in a hierarchical tree structure with grouped nodes, where wavelengths are shared both within each group and between groups at higher layers to achieve the minimum number of communication steps. To our knowledge, WRHT is the first scheme designed to optimize All-reduce operations within optical interconnect systems. This paper offers the following primary contributions:

- We propose an efficient All-reduce algorithm called WRHT to leverage the concurrent data transmission capabilities of optical interconnects. We calculate the required number of wavelengths, the minimum number of communication steps, and the optimal communication time of the All-reduce operation in an optical ring interconnect system. Our design of WRHT also considers the constraints of insertion loss and crosstalk in optical communications. In comparison with three existing All-reduce algorithms developed for electrical interconnect systems, WRHT significantly reduces the number of communication steps.
- We evaluate WRHT with comprehensive simulations. Initially, we examine the impact of varying numbers of grouped nodes and wavelengths on WRHT's performance individually, assuming they are under insertion loss and crosstalk constraints. The simulation results show that WRHT attains enhanced performance when employing a greater number of grouped nodes and wavelengths. Subsequently, we compare WRHT with three traditional All-reduce algorithms within an optical ring interconnect system with different numbers of nodes. The simulation results reveal that WRHT significantly reduces communication time by 65.23%, 43.81%, and 82.22%, respectively, when compared with three traditional All-reduce algorithms in the optical ring interconnect system.
- Lastly, we compare the All-reduce algorithm performance in optical interconnect systems to their electrical counterparts. Our results show that Ring All-reduce in the optical interconnect system achieves a 48.74% communication time reduction compared with its electrical interconnect counterpart. When compared with two traditional All-reduce algorithms in electrical interconnect system, WRHT significantly reduce the communication time for All-reduce operation by 61.23% and 55.51%, respectively.

The rest of this paper is organized as follows. Section 2 presents the related works. Section 3 illustrates the background, motivations and problem statement. Section 4 presents the WRHT scheme, including the analysis on wavelength requirement, communication steps, communication time, and constraints of optical communications. Section 5 shows the simulation results. Section 6 discusses the extension to other topologies and limitations of this paper. Finally, Section 7 concludes the paper.

2 RELATED WORK

2.1 All-reduce Optimization on Electrical Interconnect Systems

Most existing All-reduce algorithms in distributed DNN training are designed based on electrical interconnect systems. Blink [29] is a DGX-2 specific optimization designed for GPU, which uses multiple directed spanning trees to increase link utilization. Plink [15] uses a reduce/broadcast tree to balance traffic and reduce communication delay. Double binary tree (DBTree) implemented in NCCL [25] uses two-tree for reduction and broadcast respectively. A multi-tree co-design method for accelerator was proposed in [33], which can be applied to different topologies. An algorithm and network co-design method [18] is proposed to reduce the communication time of distributed DNN training by improving the bandwidth utilization on network. Other related studies include the optimization of All-reduce by reducing network contention [28], improving the performance of Ring All-reduce for large-scale clusters [8], decomposing All-reduce on heterogeneous network hierarchy [3], and adopting sparse All-reduce approach [12], etc. However, all these schemes were designed for systems using electrical networks to interconnect DNN accelerators.

2.2 Distributed Deep Learning on Optical Interconnect Systems

Nowadays, it is still in its early stage to use optical networks as the interconnect system for distributed deep learning. Only a few pieces of research work apply optical networks for distributed deep learning. A hybrid electrical-optical switch architecture for large-scale distributed deep learning was proposed in [17], achieving a 10% improvement in training time. The performance of multi-chip optical interconnect Machine-Learning architecture is evaluated in [22], and the result shows the training time is reduced by 35.6%. SiP-ML uses a strong scaling scheme for distributed machine learning training with optical interconnect [10]. Simulations show that the training time of DNN models is improved by 1.3–9.1×. However, these works focus on exploring the advantage of the high bandwidth of optical links and not on the optimization of All-reduce. Other related works include the study of all-to-all broadcast in WDM optical network [13] [23] [6], which usually formulate the routing and wavelength assignment problems as integer linear programming optimization problems without considering the special application of All-reduce operation for distributed deep learning. As far as we know, there is no existing study for optimizing All-reduce algorithms for distributed DNN training on optical interconnect system, where this study is bridging the gap.

3 BACKGROUND AND MOTIVATION

3.1 Distributed Data-parallel Training

Let us consider a DNN composed of L layers. Each layer of DNN can be either a fully connected layer or a convolutional layer. The number of neurons in layer i is represented by n_i for $i \in [1, L]$. The training of DNN consists of forward propagation (FP) and backward propagation (BP). In the forward propagation, we use $Z^{(l)}$ to represent the output vector/tensor in the layer l (input vector/tensor of layer $l+1$) and $W^{(l)}$ to represent the weight matrix at layer l. Bias vector/tensor in layer l is denoted as $B^{(l)}$. Then, the forward propagation of DNN training with n_l neurons at layer l can be defined as

$$Z^{(l)} = f(W^{(l)} Z^{(l-1)} + B^{(l)}), l = 2, 3, ..., L, \tag{1}$$

where $f(*)$ is the activation function.

In backward propagation, we define the error vector/tensor in layer l as E_l, then we get

$$E^{(l)} = (E^{(l+1)} (W^{(l)})^T) f'(Z^{(l)}), \tag{2}$$

where $f'(*)$ is the derivative function of $f(*)$.

Then, by using the error vector/tensor, the gradient of weight $\Delta W^{(l)}$ can be calculated as

$$\Delta W^{(l)} = (Z^{(l)})^T E^{(l+1)}. \tag{3}$$

After we obtain the gradient, weights are updated as follows

$$W^{(l)} = W^{(l)} + \sigma \Delta W^{(l)}, \tag{4}$$

where σ is the learning rate.

Since a convolutional layer can also be transformed into a matrix-matrix multiplication by im2col [32] with different matrix operant dimensions, the training of the convolution layer can be represented by the above equations as well.

For a distributed data-parallel DNN training, the training is paralleled among the workers by partitioning the input data across batch size b. The DNN model is replicated so that each worker maintains a local copy but has different training batches of data. In the weight update process of BP, All-reduce algorithms are used to synchronize the workers' gradients after each iteration. Assume there are n nodes in the cluster system, then the update process in data-parallel distributed DNN training equals to

$$\begin{aligned} W^{(l)} &= W^{(l)} + \sigma \Delta W^{(l)} \\ &= W^{(l)} + \frac{\sigma(\Delta W_1^{(l)} + \Delta W_2^{(l)} + ... + \Delta W_n^{(l)})}{n}. \end{aligned} \tag{5}$$

3.2 Optical Interconnect Architecture

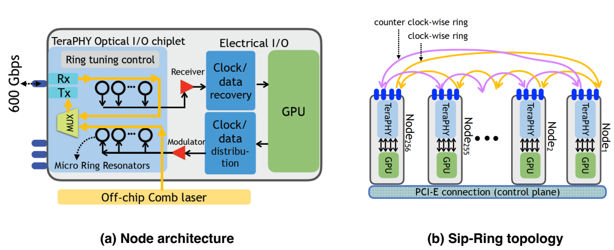

Figure 1: Optical interconnection architecture: (a) TeraRack node, (b) Double ring topology [10].

Our proposed WRHT scheme is based on an microring resonators (MRRs)-based optical switch called TeraRack [9]. However, it is worth noting that other similar optical interconnect structures, such as RAMP, could also be suitable. Figure 1 (a) shows the TeraRack node and its components based on TeraPHY silicon photonics technology. The computing component can be FPGA, TPU, GPU, and other accelerators. We assume GPU as the computing devices and GPUs are homogeneous. There are four optical interfaces on one TeraRack node with 64 micro-ring resonators to select and forward any subset of 64 wavelengths in each interface. The laser is based on a comb laser source called SuperNova Light Supply [10]. On the transmit side (Tx), an off-chip comb laser generates light that is steered into the node via a fiber coupler toward an array of MRRs modulating the accelerator's transmitting data at 40 Gbps per wavelength. On the receive side (Rx), the second array of MRRs selects the wavelengths targeted to the accelerator and passes through the remaining wavelengths. Figure 1 (b) shows the nodes interconnect with their adjacent nodes into a ring topology (only two rings for two directions are shown for clarity). In the data plane, the traffic is transmitted across four single-mode fiber rings with two clockwise rings and two counterclockwise. The Routing and Wavelength Assignment (RWA) configuration is done in the control plane, where the wavelengths can be dynamically placed around the fiber ring. This unique characteristic simplifies the control-plane logic with which datacenter optical designs have grappled for years. The details of system parameters are described in Section 5.

3.3 Motivational Study

The purpose of the All-reduce algorithm is to make every node receive the data from all the other nodes, and then apply the reduction operations (i.e., average operation) on the received data. In a general case, the All-reduce algorithm has two stages: reduce stage and broadcast stage. During reduce stage, one or a few nodes collect data from every other node and conduct the reduction operation, taking one or a few communication steps. During broadcast stage, the node(s) containing the average values broadcast the data to all the other nodes that do not have that values in a reverse direction. After that, all nodes have received the reduced value from all other nodes. We use the following motivating example to illustrate that our proposed method can significantly reduce the number of communication step for All-reduce operation to reduce the communication time. In the motivation example, we assume the system has 15 nodes based on the architecture of Figure 1 and the available number of wavelengths is two. The size of the data to reduce initially for each node is d.

Figure 2 (a) shows that binary tree (BT) All-reduce algorithm [33] consists of two stages with each stage having four steps on the 15-node network. In reduce stage, from step 1 to step 4, all nodes are divided into $\lceil N/2^i \rceil$ groups in step i. In step i, within each group, the node on the position of $2^{i-1} + 1$ sends the data of size d to the first node in a binary style (indicated by the solid arrows). At each step of reduce stage, the reduction operation is applied. During broadcast stage, from step 5 to step 8, the communications pattern is the reverse of the reduce stage (indicated by the dotted arrows). The All-reduce process is finished with all nodes receiving the reduced data. The major drawback of this method is that it only uses one wavelength during communication resulting in a large number of steps.

Figure 2 (b) shows WRHT consists of two stages on the 15-node network. The key idea of our method is to take advantage of the wavelength resources in the optical interconnect system and the two collecting directions of the ring so that the number of communication steps to realize All-reduce operation can be vastly reduced. In the first step of reduce stage, nodes are divided into three groups with the intermediate nodes responsible for collecting data within each group using two wavelengths. The reason why the representative nodes can receive the message by the same wavelength from two directions is that each node has two sets of transmitters and receivers. In the second step of reduce stage, only the three representative nodes are selected and further grouped as one group, and these three nodes exchange their data with each other using two wavelengths on the optical ring as shown in Figure 2 (b). So far, the representative nodes have received the average values of all nodes and will broadcast the average values to other nodes in the broadcast stage. During the broadcast stage, since all the three representative nodes now have the reduction data, they broadcast the data within each group using two wavelengths in just one step, as shown in step 3 of Figure 2 (b). Since reduction operation is applied during every step of the reduce stage, the size of transferred data is d (a constant value) in both reduce stage and broadcast stage. Therefore, WRHT can effectively reduce the number of communication steps, so that the communication time for All-reduce operation can be largely reduced.

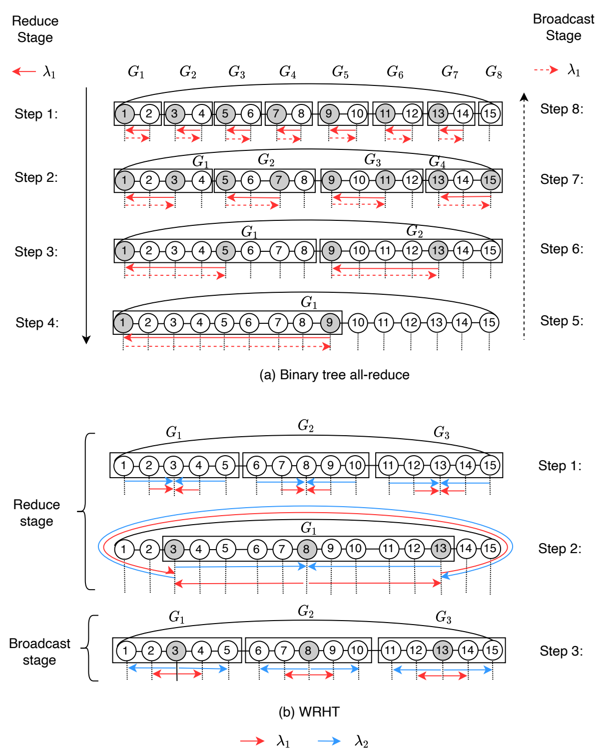

Figure 2: All-reduce algorithm: (a) Binary tree (8 steps), (b) WRHT (3 Steps), © 2023 Fei Dai.

3.4 Problem Definition

Through the motivation example, we know that the existing All-reduce algorithms on electrical interconnect systems cannot take advantage of the optical interconnection system's optical resources to reduce the number of communication steps. We need an efficient All-reduce algorithm for optical systems to minimize communication steps and time. The challenging problem is: *How to design an efficient routing scheme in optical interconnect system for All-reduce that can utilize multiple wavelengths in each communication step to minimize the total communication time?* Given the constant communication quantity of All-reduce, with transferred data size d per step, the problem becomes designing an All-reduce routing scheme to minimize total communication steps. This paper's goal is to design an efficient All-reduce routing scheme for an optical interconnect system, minimizing total communication steps.

4 THE WRHT SCHEME

In this section, we first describe the design of WRHT including the routing and wavelength assignment. Then, we analyze the communication steps of WRHT and several All-reduce algorithms and derive the optical communication time of the All-reduce operation. Finally, we discuss the constraints of optical communications.

4.1 Design of WRHT

4.1.1 Routing Algorithm Design. We assume there are N computing nodes, and the computing node can be GPU, TPU, NPU, etc. The number of available wavelengths per waveguide is w and the bandwidth per wavelength is B. We use Figure 3 to illustrate the mechanism of WRHT, which consists of two stages: reduce stage and broadcast stage.

Reduce stage: In step 1, all nodes are partitioned into groups along the ring with each group having m nodes. The intermediate node of each group is selected as the representative node and responsible for collecting the data within each group by $\lfloor m/2 \rfloor$ wavelengths. After that, each representative node executes a reduction operation to be transmitted in the next step. In the subsequent step i, the old representative nodes selected in the previous step are further partitioned into $\lceil \frac{N}{m^i} \rceil$ groups and the middle node of each group is selected as the new representative node as illustrated in Figure 3. This process is repeated until the wavelength is sufficient enough to provide all-to-all communication among the representative nodes in the last step, as illustrated by the dotted box in the middle of Figure 3.

Broadcast stage: Once the representative node(s) in the final step of reduce stage obtain the final reduction value, the process of broadcast stage is the reverse of reduce stage. Specifically, the representative nodes broadcast the reduction data in corresponding groups using $\lfloor m/2 \rfloor$ wavelengths, which is repeated according to the hierarchical tree structure until all the nodes receive the reduce data, as illustrated in the lower part of Figure 3. The total number of communication steps are discussed in Section 4.2.

4.1.2 Wavelength Requirement. In the WRHT algorithm, nodes are partitioned into subgroups at each step, necessitating proper wavelength assignment within each subgroup to prevent conflicts. Communications from different subgroups are independent, allowing for wavelength reuse within subgroups. Thus, we can employ the like First Fit [21] or Random Fit [31] wavelength assignment approaches for each subgroup. Given that there are m nodes in each subgroup and an intermediate node is selected as the representative node, the

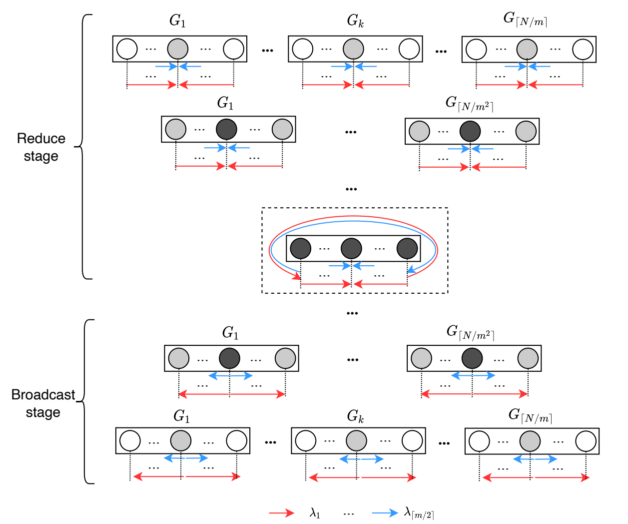

Figure 3: The working principle in WRHT scheme, © 2023 Fei Dai.

wavelength requirement can be easily deduced as $\lfloor m/2 \rfloor$. For the last step in reduce stage, the number of representative nodes can be derived as $m^* = \lceil \frac{N}{m^{\lceil log_m N \rceil - 1}} \rceil$, which requires $\lceil \frac{(m^*)^2}{8} \rceil$ wavelengths for all-to-all communications [13] when $m^* > 1$.

4.2 Analysis of Communication Steps

The total DNN training time is dominated by the number of communication steps since MRRs should be reconfigured before each communication step and the amount of data traffic in each communication step is constant. Therefore, we analyze the number of communication steps of WRHT and compare it with other existing All-reduce algorithms. Based on the hierarchical tree structure with m nodes in each subgroup, WRHT requires $\lceil \log_m N \rceil$ steps in the reduce stage. If the all-to-all broadcast among representative nodes is involved in the last step of reduce stage, the broadcast stage requires $\lceil \log_m N \rceil - 1$ steps. Otherwise, the number of steps in the broadcast stage is $\lceil \log_m N \rceil$. As a result, the total number of communication steps for WRHT is $2\lceil \log_m N \rceil$ or $2\lceil \log_m N \rceil - 1$. For traditional BT All-reduce, $\lceil \log_2 N \rceil$ steps are required in both reduce stage and broadcast stage. For traditional Ring All-reduce, it takes $2(N-1)$ steps for the gradient synchronization. Another traditional H-Ring All-reduce algorithm [28] requires $\frac{2(m^2+N)}{m} - 3$ steps ($\lceil \frac{m}{w} \rceil = 1$) or $\frac{2(2m^2+N)}{m} - 6$ steps ($\lceil \frac{m}{w} \rceil > 1$), where m is the number of intra-group nodes and w is the available number of wavelengths. We summarize the comparison on the communication steps of these classic All-reduce algorithms and WRHT in Table 1.

4.3 Communication Time of WRHT

The communication time of WRHT includes the communication time for reduce stage T_{reduce} and broadcast stage T_{bcast}. We denote a as the delay of O/E/O conversion and reconfiguration delay of the MRRs, B as the bandwidth per wavelength and d as the size of transferred data to be reduced initially for each node. Thus, the

Table 1: Communication step comparison for different All-reduce algorithms in optical interconnect system.

Algorithm	Communication steps	Number of steps
		N = 1024, w = 64
Ring	$2(N-1)$	2046
H-Ring	$\frac{2(m^2+N)}{m} - 3$ ($\lceil \frac{m}{w} \rceil = 1$) or $\frac{2(2m^2+N)}{m} - 6$ ($\lceil \frac{m}{w} \rceil > 1$)	417 (m=5)
BT	$2\lceil \log_2 N \rceil$	20
WRHT	$2\lceil \log_m N \rceil$ or $2\lceil \log_m N \rceil - 1$	3 (m = 129)

communication time of WRHT, denoted as T_{comm}, can be calculated as:

$$\begin{aligned} T_{comm} &= T_{reduce} + T_{bcast} \\ &= \frac{d\theta}{B} + a\theta, \end{aligned} \tag{6}$$

where θ represents the total number of communication steps and $\theta = 2\lceil \log_m N \rceil$ or $2\lceil \log_m N \rceil - 1$. We further derive the minimum number of communication steps and optimal communication time to realize the All-reduce operation on optical ring system as shown in the following results.

LEMMA 1. *In an N-node optical ring interconnect system with w available wavelengths, the lower bound on the number of communication steps by WRHT for finishing the All-reduce operation is* $2\lceil \log_{2w+1} N \rceil$.

PROOF. As the total number of communication steps is at most $\theta = 2\lceil \log_m N \rceil$, which is decreasing with the increasing number of nodes m in each subgroup. Given w available wavelengths, the maximum number of nodes that can be selected for each subgroup is $m = 2w + 1$. Therefore, the lower bound on the number of communication steps by WRHT for finishing the All-reduce operation is $2\lceil \log_{2w+1} N \rceil$. □

THEOREM 1. *In an N-node optical ring interconnect system with w available wavelengths, the lower bound on the communication time by WRHT for distributed DNN training is* $\frac{2d\lceil \log_m N \rceil}{B} + 2a\lceil \log_m N \rceil$.

PROOF. It can be seen from Equation (6) that the parameters of d, B, and a are all constant values. The optimal communication time using WRHT can be achieved when the number of communication steps for All-reduce operation θ is minimized. According to Lemma 1, the lower bound of communication time is $\frac{2d\lceil \log_m N \rceil}{B} + 2a\lceil \log_m N \rceil$ for distributed DNN training in an N-node optical ring interconnect system with w available wavelengths. □

4.4 Constraints of Optical Communications

Challenges such as insertion loss and crosstalk arise in optical communication when optical signals traverse through optical interfaces. As such, we discuss the implications of these issues and the constraints they place on our proposed WRHT scheme.

4.4.1 Insertion Loss. Insertion loss occurs when optical signals traverse optical interfaces. To discuss the constraint for the maximum optical communication length, we calculate the maximum number of grouped nodes, denoted as m'. It is important to note that using a different number of grouped nodes in the initial step can result in varying hierarchical levels, leading to different communication lengths. Thus, given the total number of nodes and grouped nodes for the first step, we can determine the maximum communication length L_{max} for the WRHT by

$$L_{max} = \begin{cases} \left\lfloor \frac{m'}{2} \right\rfloor, \log_{m'} N = 1; \\ m'(m'^{\log_{m'} N-2}), \log_{m'} N \geq 2. \end{cases} \tag{7}$$

Given the maximum communication length L_{max} of WRHT and signal loss for the signal past an interface P_{pass}, we can derive the total optical loss L_l by

$$L_l = P_m + L_{max} P_{pass}, \tag{8}$$

where P_m is the modulator loss in the Tx.

According to [14], the optical power constraint for the laser source power P_{laser}, total optical insertion loss L_l, and the power penalty caused by extinction ratio P_p can be represented as

$$P_{laser} \geq L_l + P_p. \tag{9}$$

Since P_m, P_p, P_{pass} are known system parameters, we can estimate the maximum number of grouped nodes m' according to equations (7), (8), and (9). Therefore, the number of grouped nodes m is no larger than m':

$$m \leq m'. \tag{10}$$

4.4.2 Crosstalk. Crosstalk in optical communication refers to the unintended detection of a signal by an adjacent wavelength, which causes interference and signal quality degradation. The effect of crosstalk noise in the optical interconnect system can be quantified using the signal-to-noise ratio (SNR). SNR can be mathematically expressed as

$$\mathrm{SNR} = 10 \log \frac{P_S}{P_N + P_O}, \tag{11}$$

where P_S denotes the optical signal power, P_N represents the crosstalk noise power received at the photodetector in the receiver, and P_O refers to the power of other noise sources present in the system.

The worst-case crosstalk noise power, P_{N_w}, is primarily dominated by the worst-case crosstalk noise power on the Tx side (P_{Tx}) and the worst-case crosstalk noise power on the Rx side (P_{Rx}) during optical communication. It can be estimated by

$$P_{N_w} = L_{max} P_{Rx} + P_{Tx}. \tag{12}$$

The bit-error-rate (BER) represents the percentage of bits with errors among the total number of bits received during a transmission. It is utilized as a criterion to evaluate the quality of optical communication [26]. The relationship between BER and $\mathrm{SNR_w}$ in the optical interconnect system is

$$\mathrm{BER} = \frac{1}{2} e^{-\frac{\mathrm{SNR_w}}{4}}. \tag{13}$$

To ensure reliable transmissions in an optical interconnect system, the BER must be lower than 10^{-9}[26]. Using equations (11), (12), and (13), we can estimate the optical laser power P_S required to achieve reliable optical communications for DNN training. The system needs to satisfy the crosstalk and laser power constraints.

5 EVALUATIONS

5.1 Implementation

To simulate the communications of distributed DNN training in an optical interconnect system, we employ an in-house optical interconnect system simulator that implements WRHT and other All-reduce algorithms. Traditional datacenter clusters with electrical packet switches are arranged in a multi-layer Fat-tree topology, and today's DNN training is built on top of it [30]. We utilize the SimGrid framework version 3.3 discrete-event simulator [2] for simulating the Fat-tree electrical interconnect system. In our simulations, we assume the use of float32 data type for operations and GPUs as accelerators in both electrical and optical systems.

To evaluate the performance of WRHT, we use a variety of DNN workloads that can fit in the GPU memory, as distributed data-parallel training requires each GPU to maintain a copy of the DNN model. These workloads include the transformer model BEiT-L [1] (307M parameters), and three standard CNN models such as VGG16 (138M parameters), AlexNet (62.3M parameters), and ResNet50 (25M parameters) with the MNIST and ImageNet datasets [11].

To enhance the simulation's credibility, we first profile DNN workloads on a server with four machines, each with an Intel i7-6700K 4.0 GHz CPU, 64GB RAM, and two GeForce GTX TITAN XP GPUs. We measure average GPU and CPU computation times, peak memory sizes, and total data transfer sizes during backpropagation using TensorFlow profiler. We find that different applications or datasets affect only the total training time, not the All-reduce performance, as the size of transferred data in distributed data-parallel training remains nearly constant given the same batch size. We then use the size of transferred data as input for both our optical interconnect simulator and the electrical interconnect simulator SimGrid.

To ensure a fair comparison between electrical and optical interconnect systems, we set identical packet sizes and delays for both. The parameters for both optical interconnect and electrical interconnect systems used in our simulations are detailed in Table 2, with optical interconnect parameters sourced from [10] [5]. In the simulation, communication time is estimated by numerically calculating the number of parameters in our simulator and SimGrid. Specifically, we vary the number of nodes in SimGrid, using the transferred data sizes of DNN models to obtain the communication time of the electrical interconnect system. The All-reduce benchmark for different sizes of transferred data in this SimGrid resembles [19]. For the optical interconnect system, we input the size of DNN parameters and the number of nodes into our in-house optical interconnect system simulator to determine the communication time of various All-reduce algorithms. The communication time evaluation is based on one epoch of training time since the training is repeated.

5.2 Experiment Setup

We compare WRHT with four All-reduce algorithms in our experiments: Ring, H-Ring, BT, and Recursive Doubling (RD). Ring, H-Ring, and BT serve as baselines in the optical interconnect system, while Ring and RD are used as baselines in the comparison between electrical and optical interconnect systems.

Table 2: Parameters of simulated architecture

Interconnect	Parameters setup
Electrical network	Fat-tree topology, Two-level cluster with 32 port routers, Router full bisection bandwidth: 40 Gbps, Router delay: 25 μs, Packet size: 72 bytes, Shortest-path routing.
Optical network	Double ring, 64 wavelengths, MRRs reconfiguration delay: 25 μs, O/E/O conversion delay: 497 fs/packet, Packet size: 72 bytes, 40 Gbps/wavelength.

We conduct the following experiments to test the performance of WRHT:

(1) We evaluate WRHT in a 1024-node optical interconnect system by setting up various numbers of grouped nodes, assuming they satisfy the insertion loss and crosstalk constraints.
(2) We test WRHT's performance using different numbers of wavelengths.
(3) We compare WRHT with traditional All-reduce algorithms in optical interconnect systems with varying node counts.
(4) We compare the performance of All-reduce algorithms between electrical and optical interconnect systems across different numbers of nodes.

5.3 Performance Test with Different Numbers of Grouped Nodes in WRHT

Since the constraints of optical communication (discussed in Section 4.4) will restrict the number of grouped nodes m in WRHT, we first test the performance differences of WRHT with different numbers of grouped nodes on a 1024-node optical interconnect system. We set the numbers of grouped nodes in WRHT as 17, 33, 65, and 129, assuming they are the number of grouped nodes under insertion loss and crosstalk constraints. To differentiate different settings, we name WRHT with 17, 33, 65, and 129 numbers of grouped nodes settings as $WRHT_0$, $WRHT_1$, $WRHT_2$, and $WRHT_3$. The DNN workloads used in the simulation are set with corresponding batch sizes that fully utilize GPU memory for All-reduce algorithms. All results in Figure 4 are normalized by dividing the result of $WRHT_3$ in each DNN workload.

Figure 4 illustrates the performance of WRHT on a 1024-node optical interconnect system with different numbers of grouped nodes using different DNN workloads. From Figure 4, we can see that with the increasing number of grouped nodes, the communication time keeps decreasing and then keeps still. That is because the communication time of WRHT is mainly decided by the number of communication steps according to Equation (6). With the increasing number of grouped nodes in the WRHT, the number of communication steps decreases and then keeps still. Besides, we notice that the communication time of $WRHT_2$ and $WRHT_3$ are only half of $WRHT_0$ regardless of DNN workloads. That is because the optical interconnect system is based on circuit switching and conducts concurrent communication via WDM. Therefore, it is free from network congestion of electrical network and performs similarly with different amounts of transferred data. In conclusion, using a large number of grouped nodes in WRHT can perform better.

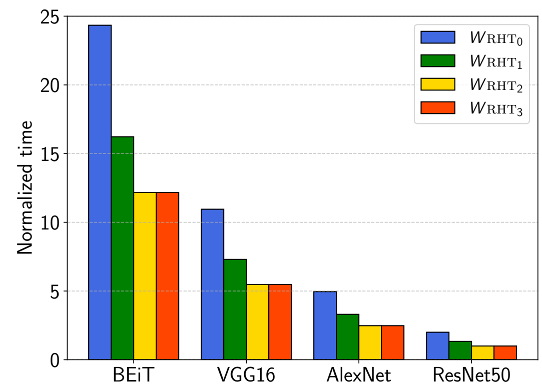

Figure 4: Performance test with different numbers of grouped nodes in WRHT on 1024-node optical interconnect system.

5.4 Impact of Number of Wavelengths

Since wavelengths are important resources in optical interconnect system, we first test the performance of WRHT on a 1024-node optical interconnect system by using 4, 16, 64, and 256 wavelengths compared with Ring, H-Ring, and BT All-reduce algorithms. In the simulation, we set the number of nodes in the group for H-Ring is 5 and assume there is no constraint of optical communication for WRHT in the simulation. Besides, the DNN workloads used in the simulation are set with corresponding batch sizes that fully utilize GPU memory for All-reduce algorithms using tuning method. All results in Figure 5 are normalized by dividing the result of WRHT in ResNet50 with 256 wavelengths.

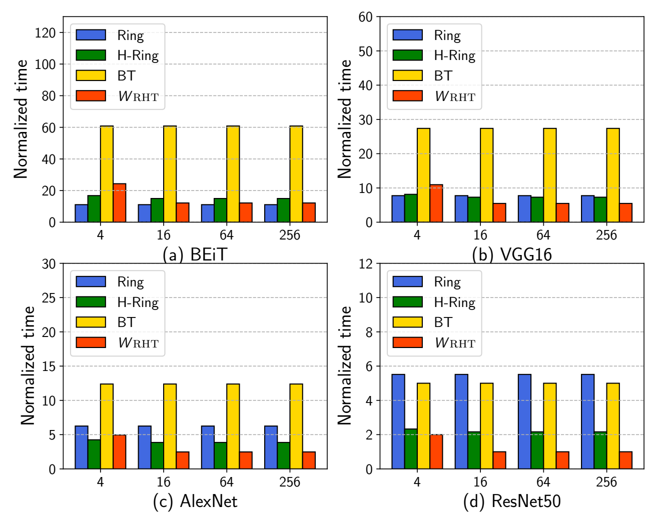

Figure 5: Comparison of communication time of four algorithms in the 1024-node optical interconnect system under different wavelengths.

Figure 5 shows the comparison of communication time between WRHT and three All-reduce algorithms on a 1024-node optical interconnect system using 4, 16, 64, and 256 wavelengths. From Figure 5 (a) to (d), we can see that the total communication time of WRHT first decrease and then keep constant with the increasing number of wavelengths. The reason is that communication time of WRHT is proportional to the number of communication steps. With the increasing number of wavelengths according to Equation (6), the number of communication steps in WRHT first decreases but keeps still because the number of wavelengths cannot further reduce the number of communication steps in WRHT. The Figure 5 also shows the total communication time of the H-Ring slightly decreases after wavelength four and keeps constant for the four DNNs with the increasing number of wavelengths. That is because number of grouping node m is set to 5, and when the wavelength increases, the number of communication step decreases. The calculation of the number of communication steps in the H-Ring can refer to in Table 1. From Figure 5 (a) to (d), we can also see that the communication time of Ring and BT is constant with the increasing number of wavelengths. That is because both the All-reduce algorithms do not take advantage of the wavelength and use only one wavelength along the optical link. We also notice that in Figure 5 (b) WRHT does not perform well compared with Ring and H-Ring when using four wavelengths for transferring the amounts of data in BEiT and VGG16. The reason is that when the number of wavelengths is small, the number of communication steps in WRHT increases, and the transferred data size of each step is d for the All-reduce operation. Although Ring takes $2(n-1)$ steps to finish the All-reduce operation, the transferred data size of each step is $\frac{d}{n}$. That explains why WRHT does not perform well when the number of wavelength is small and with a large amount of transferred data. Overall, unlike traditional All-reduce algorithms, the communication time of WRHT decreases effectively with the increasing number of wavelengths. Compared with Ring, H-Ring, and BT, the WRHT reduces communication time by 13.74%, 9.29%, and 75% on average, respectively.

5.5 Comparison of Traditional All-reduce Algorithms on Optical Interconnect System

Considering the current scale in the cluster, we compare WRHT with Ring, H-Ring, and BT All-reduce in the optical interconnect system by setting 1024, 2048, 3072, 4096 nodes respectively. The simulation setup is the same as the previous section, except that we use 64 wavelengths and vary the number of nodes in the optical interconnect system. All results in Figure 6 are normalized by dividing the first result of WRHT in ResNet50.

Figure 6 presents a comparison of communication time between WRHT and three traditional All-reduce algorithms across different DNN models. From Figure 6 (a) to (d), it is evident that the total communication time of WRHT is the lowest for all DNN models, and the communication time remains nearly constant as the number of nodes increases from 1024 to 4096. This is because WRHT can achieve the lower bound for both the number of communication steps and communication time, as demonstrated in Lemma 1 and Theorem 1. As the number of nodes grows, the communication time for BT shows a slight overall increase, but its performance varies significantly among different DNNs. Specifically, BT performs well for DNNs with smaller transfer data sizes, such as ResNet50, but struggles with DNNs involving larger amounts of transferred data, like BEiT, VGG16, and AlexNet. In particular, BT's communication time in BEiT and VGG16 is the worst among all All-reduce algorithms, regardless of the number of nodes. In contrast, the other two ring-based All-reduce algorithms both exhibit an increasing trend in communication time as the number of GPU nodes grows. However, the communication time for Ring exhibits a linear rise with increasing cluster size, while the growth of H-Ring's communication time is comparatively slower. The reason for the observed trends in communication time for Ring and H-Ring is that both algorithms exhibit a linear increase in the number of communication steps as the number of nodes grows, but H-Ring has fewer communication steps. Although the size of transferred data for ring-based algorithms is $\frac{d}{n}$ compared with the size of transferred data d in both BT and WRHT, the communication time for distributed DNN training is primarily determined by the number of communication steps. The comparison with these three traditional algorithms highlights that different All-reduce algorithms result in varying numbers of steps and amounts of transmitted data. The communication time of All-reduce depends on the amount of transmitted data and the required number of steps in the transmission process. In comparison to Ring, H-Ring, and BT, WRHT reduces communication time by 65.23%, 43.81%, and 82.22% on average, respectively, demonstrating its superior performance.

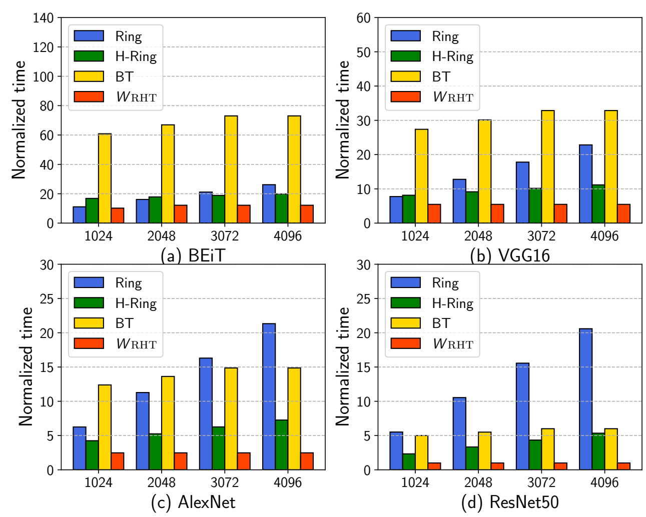

Figure 6: Comparison of communication time in optical interconnect system using different All-reduce algorithms under different numbers of nodes.

5.6 Performance Comparison Between Optical Interconnect and Electrical Interconnect System

We compare the performance of All-reduce algorithms between the electrical and optical interconnect systems for four DNNs with 128, 256, 512, and 1024 nodes, respectively. In the electrical interconnect system, we use the common fat-tree topology found in datacenters and deploy Ring and Recursive Doubling (RD) All-reduce algorithms. On the other hand, we deploy Ring All-reduce algorithm and Wrht in the optical ring interconnect system with 64 wavelengths. To easily distinguish the communication time obtained by the Ring All-reduce algorithm on different platforms, we name the algorithm in the electrical interconnect system as E-Ring, and the one running in the optical interconnect system as O-Ring. All results in Figure 7 are normalized by dividing the result of Wrht in ResNet50.

Figure 7 compares the communication time of Ring and RD All-reduce algorithms in the electrical interconnect system with Ring All-reduce and Wrht in the optical interconnect system across different DNN models and scales. From Figure 7 (a) to (d), we observe that the communication time of Wrht is the lowest and increases only slightly with the growing number of nodes. The rest of the All-reduce algorithms in both optical and electrical interconnect systems exhibit an increasing trend as the cluster scales. The communication time of the Ring All-reduce algorithm in the electrical interconnect system is the highest, while the communication time of the RD All-reduce is slightly lower. When comparing the Ring All-reduce algorithm between the optical and electrical interconnect systems, we find that O-Ring significantly reduces communication time compared with E-Ring. This performance gain for the Ring All-reduce algorithm in the optical interconnect system results from the absence of routing congestion in circuit-switching optical interconnects. Furthermore, the bandwidth bottleneck in the electrical interconnect system lies in the routers, where packets from all nodes must pass through two levels of routers for data transmission. In contrast, communication between nodes in the optical interconnect can use bandwidth exclusively, further enhancing its performance. Overall, the communication time of Ring All-reduce in the optical interconnect system achieves an average reduction of 48.74% compared with the electrical interconnect system. Comparing Wrht with Ring and RD All-reduce algorithms in the electrical interconnect system, the communication time is reduced by 61.23% and 55.51%, respectively. These results demonstrate the significant performance improvements offered by Wrht in the optical interconnect system compared with traditional All-reduce algorithms in both optical and electrical systems.

6 DISCUSSION

6.1 Extension to Other Topologies

While Wrht is specifically designed for optical interconnect systems with ring topology, its principles can be extended to other topologies such as mesh and torus. To illustrate, let's consider the application of Wrht to a torus topology. Assume an $n \times n$ torus; we can first apply the reduce stage of Wrht to each row of the torus, provided $m \leq n$. Subsequently, the representative nodes in each row synchronize with one another. The broadcast stage then proceeds in reverse order of the reduce stage. The Wrht concept can similarly be applied to a mesh topology, with the key difference being that the one-stage model for a line [13] is employed in the final stage, rather than the one-stage model for a ring. Overall, the All-reduce process of Wrht in torus or mesh topologies is considerably simpler, given that the row and column sizes of the torus or mesh are n.

6.2 Limitations

It is essential to acknowledge the limitations of our paper. Due to the lack of a formal optical interconnect simulator for distributed DNN training, we employ our in-house optical interconnect simulator to model the communication of various All-reduce algorithms in distributed data-parallel DNN training. Our simulations focus solely on the communication time of All-reduce in the simulated optical interconnect system. A more in-depth analysis of communication time for optical interconnect systems would necessitate a hardware-specific execution model, which is beyond the scope of this study.

The primary contribution of our paper lies in the creation of the All-reduce algorithm, Wrht, not the development of an optical interconnect system. The cost aspect is not covered in this paper, as the TeraRack architecture has already showcased substantial cost savings in comparison to its counterparts. Specifically, it offers a 6× reduction in cost compared to electrical interconnects and a 4× reduction in comparison to other optical interconnects, as reported in [9]. We have taken into account insertion loss and crosstalk in optical communications for Wrht and have extensively tested the algorithm, finding that grouping a larger number of nodes and using more wavelengths lead to better performance. As optical integration technology advances, we expect the insertion loss and crosstalk in optical interconnect systems to decrease further, thereby enhancing Wrht's performance. Importantly, although Wrht is based on TeraRack, it remains versatile enough for implementation in other optical interconnect systems such as RAMP.

Additionally, our simulations consider various DNN models, such as BEiT, VGG16, AlexNet, and ResNet50. Theoretically, Wrht is applicable to any neural network, provided that the memory can store the entire DNN model during the distributed data-parallel DNN training. Large language models (LLMs) like GPT3 necessitate alternative parallel methods, including model-parallel, pipeline-parallel, or hybrid-parallel approaches, as a processing node in distributed data-parallel training cannot accommodate GPT3 in its

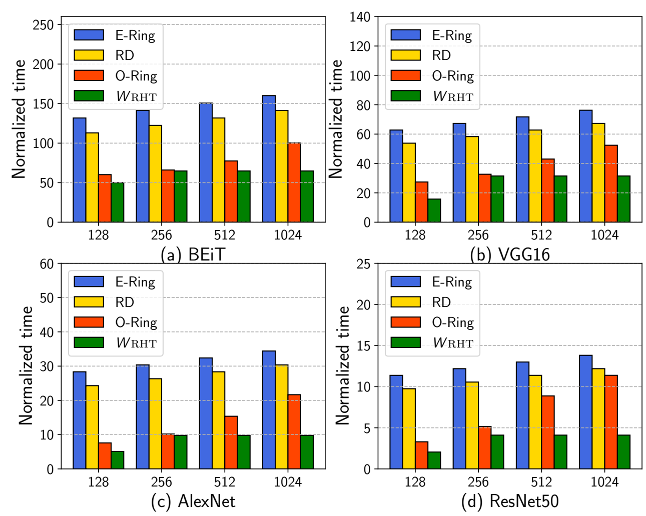

Figure 7: Comparison of communication time in electrical and optical interconnect systems with different All-reduce algorithms and numbers of nodes.

memory. WRHT can also be employed during LLM training in an optical interconnect system when using model-parallel, pipeline-parallel, or hybrid-parallel methods. Nonetheless, training LLMs in optical interconnect systems using other parallel methods that invoke WRHT remains an area for future exploration.

7 CONCLUSION

In this paper, we introduce WRHT, an efficient All-reduce scheme tailored for distributed data-parallel DNN training in optical interconnect systems. The primary objective of WRHT is to minimize communication time. Our approach derives the required number of wavelengths, the minimum number of communication steps, the optimal communication time for the All-reduce operation, and the constraints of optical communications within the optical ring interconnect system. Simulation results demonstrate that WRHT outperforms traditional All-reduce algorithms in optical interconnect systems, reducing communication time by an average of 65.23%, 43.81%, and 82.22% compared with three different algorithms. Furthermore, when compared with two All-reduce algorithms implemented in electrical interconnect systems, WRHT achieves an average communication time reduction of 61.23% and 55.51%. Future work can be done by extending our work to other interconnect topologies and heterogeneous computing device scenarios.

REFERENCES

[1] Hangbo Bao, Li Dong, Songhao Piao, and Furu Wei. 2022. BEiT: BERT Pre-Training of Image Transformers. In *International Conference on Learning Representations*. https://openreview.net/forum?id=p-BhZSz59o4

[2] Henri Casanova, Arnaud Legrand, and Martin Quinson. 2008. Simgrid: A generic framework for large-scale distributed experiments. In *Tenth International Conference on Computer Modeling and Simulation (uksim 2008)*. IEEE, 126–131.

[3] Minsik Cho, Ulrich Finkler, Mauricio Serrano, David Kung, and Hillery Hunter. 2019. BlueConnect: Decomposing all-reduce for deep learning on heterogeneous network hierarchy. *IBM Journal of Research and Development* 63, 6 (2019), 1–1.

[4] Fei Dai, Yawen Chen, Zhiyi Huang, Haibo Zhang, and Fangfang Zhang. 2023. Efficient All-Reduce for Distributed DNN Training in Optical Interconnect Systems. In *Proceedings of the 28th ACM SIGPLAN Annual Symposium on Principles and Practice of Parallel Programming*. 422–424.

[5] Fei Dai, Yawen Chen, Zhiyi Huang, Haibo Zhang, Hao Zhang, and Chengpeng Xia. 2023. Comparing the performance of multi-layer perceptron training on electrical and optical network-on-chips. *The Journal of Supercomputing* 79, 10 (2023), 10725–10746.

[6] Qian-Ping Gu and Shietung Peng. 2003. Multihop all-to-all broadcast on WDM optical networks. *IEEE Transactions on Parallel and Distributed Systems* 14, 5 (2003), 477–486.

[7] Jiayi Huang, Pritam Majumder, Sungkeun Kim, Abdullah Muzahid, Ki Hwan Yum, and Eun Jung Kim. 2021. Communication Algorithm-Architecture Co-Design for Distributed Deep Learning. In *2021 ACM/IEEE 48th Annual International Symposium on Computer Architecture (ISCA)*. IEEE, 181–194.

[8] Youhe Jiang, Huaxi Gu, Yunfeng Lu, and Xiaoshan Yu. 2020. 2D-HRA: Two-Dimensional Hierarchical Ring-Based All-Reduce Algorithm in Large-Scale Distributed Machine Learning. *IEEE Access* 8 (2020), 183488–183494.

[9] Mehrdad Khani, Manya Ghobadi, Mohammad Alizadeh, Ziyi Zhu, Madeleine Glick, Keren Bergman, Amin Vahdat, Benjamin Klenk, and Eiman Ebrahimi. 2020. Terarack: A tbps rack for machine learning training. (2020).

[10] Mehrdad Khani, Manya Ghobadi, Mohammad Alizadeh, Ziyi Zhu, Madeleine Glick, Keren Bergman, Amin Vahdat, Benjamin Klenk, and Eiman Ebrahimi. 2021. SiP-ML: high-bandwidth optical network interconnects for machine learning training. In *Proceedings of the 2021 ACM SIGCOMM 2021 Conference*. 657–675.

[11] S. T. Krishna and H. K. Kalluri. 2019. Deep learning and transfer learning approaches for image classification. *International Journal of Recent Technology and Engineering (IJRTE)* 7, 5S4 (2019), 427–432.

[12] Shigang Li and Torsten Hoefler. 2022. Near-optimal sparse allreduce for distributed deep learning. In *Proceedings of the 27th ACM SIGPLAN Symposium on Principles and Practice of Parallel Programming*. 135–149.

[13] Weifa Liang and Xiaojun Shen. 2006. A general approach for all-to-all routing in multihop WDM optical networks. *IEEE/ACM transactions on networking* 14, 4 (2006), 914–923.

[14] Heng Liao, Jiajin Tu, Jing Xia, Hu Liu, Xiping Zhou, Honghui Yuan, and Yuxing Hu. 2021. Ascend: a scalable and unified architecture for ubiquitous deep neural network computing: Industry track paper. In *2021 IEEE International Symposium on High-Performance Computer Architecture (HPCA)*. IEEE, 789–801.

[15] Liang Luo, Peter West, Jacob Nelson, Arvind Krishnamurthy, and Luis Ceze. 2020. Plink: Discovering and exploiting locality for accelerated distributed training on the public cloud. *Proceedings of Machine Learning and Systems* 2 (2020), 82–97.

[16] Ruben Mayer and Hans-Arno Jacobsen. 2020. Scalable deep learning on distributed infrastructures: Challenges, techniques, and tools. *ACM Computing Surveys (CSUR)* 53, 1 (2020), 1–37.

[17] Truong Thao Nguyen and Ryousei Takano. 2019. On the feasibility of hybrid electrical/optical switch architecture for large-scale training of distributed deep learning. In *2019 IEEE/ACM Workshop on Photonics-Optics Technology Oriented Networking, Information and Computing Systems (PHOTONICS)*. IEEE, 7–14.

[18] Truong Thao Nguyen and Mohamed Wahib. 2021. An Allreduce Algorithm and Network Co-design for Large-Scale Training of Distributed Deep Learning. In *2021 IEEE/ACM 21st International Symposium on Cluster, Cloud and Internet Computing (CCGrid)*. IEEE, 396–405.

[19] Truong Thao Nguyen, Mohamed Wahib, and Ryousei Takano. 2018. Hierarchical distributed-memory multi-leader mpi-allreduce for deep learning workloads. In *2018 Sixth International Symposium on Computing and Networking Workshops (CANDARW)*. IEEE, 216–222.

[20] Alessandro Ottino, Joshua Benjamin, and Georgios Zervas. 2022. RAMP: A Flat Nanosecond Optical Network and MPI Operations for Distributed Deep Learning Systems. *arXiv preprint arXiv:2211.15226* (2022).

[21] Asuman E Ozdaglar and Dimitri P Bertsekas. 2003. Routing and wavelength assignment in optical networks. *IEEE/ACM transactions on networking* 11, 2 (2003), 259–272.

[22] Yuhwan Ro, Eojin Lee, and Jung Ho Ahn. 2018. Evaluating the Impact of Optical Interconnects on a Multi-Chip Machine-Learning Architecture. *Electronics* 7, 8 (2018), 130.

[23] M Sabrigiriraj and M Meenakshi. 2008. All-to-all broadcast in optical WDM networks under light-tree model. *Computer communications* 31, 10 (2008), 2562–2565.

[24] Paul Sack and William Gropp. 2012. Faster topology-aware collective algorithms through non-minimal communication. *ACM SIGPLAN Notices* 47, 8 (2012), 45–54.

[25] Peter Sanders, Jochen Speck, and Jesper Larsson Träff. 2009. Two-tree algorithms for full bandwidth broadcast, reduction and scan. *Parallel Comput.* 35, 12 (2009), 581–594.

[26] Santu Sarkar and Nikhil R Das. 2009. Study of component crosstalk and obtaining optimum detection threshold for minimum bit-error-rate in a WDM receiver. *Journal of lightwave technology* 27, 19 (2009), 4366–4373.

[27] N Terzenidis, G Giamougiannis, A Tsakyridis, D Spasopoulos, F Yan, N Calabretta, C Vagionas, and N Pleros. 2021. Performance analysis of a 1024-port Hipoλaos OPS in DCN, HPC, and 5G fronthauling Ethernet applications. *Journal of Optical Communications and Networking* 13, 7 (2021), 182–192.

[28] Yuichiro Ueno and Rio Yokota. 2019. Exhaustive study of hierarchical allreduce patterns for large messages between gpus. In *2019 19th IEEE/ACM International Symposium on Cluster, Cloud and Grid Computing (CCGRID)*. IEEE, 430–439.

[29] Guanhua Wang, Shivaram Venkataraman, Amar Phanishayee, Nikhil Devanur, Jorgen Thelin, and Ion Stoica. 2020. Blink: Fast and generic collectives for distributed ml. *Proceedings of Machine Learning and Systems* 2 (2020), 172–186.

[30] Weiyang Wang, Moein Khazraee, Zhizhen Zhong, Manya Ghobadi, Zhihao Jia, Dheevatsa Mudigere, Ying Zhang, and Anthony Kewitsch. 2023. {TopoOpt}: Co-optimizing Network Topology and Parallelization Strategy for Distributed Training Jobs. In *20th USENIX Symposium on Networked Systems Design and Implementation (NSDI 23)*. 739–767.

[31] Amit Wason and RS Kaler. 2011. Wavelength assignment algorithms for WDM optical networks. *Optik* 122, 10 (2011), 877–880.

[32] Jinghe Wei, Younis Ibrahim, Siyu Qian, Haibin Wang, Guozhu Liu, Qingkui Yu, Rong Qian, and Junwei Shi. 2020. Analyzing the impact of soft errors in VGG networks implemented on GPUs. *Microelectronics Reliability* 110 (2020), 113648.

[33] Carl Yang and AWS Amazon. 2018. Tree-based Allreduce Communication on MXNet. *Tech. Rep.* (2018).

[34] Peng Yang, Zhehui Wang, Zhifei Wang, Jiang Xu, Yi-Shing Chang, Xuanqi Chen, Rafael KV Maeda, and Jun Feng. 2019. Multidomain Inter/Intrachip Silicon Photonic Networks for Energy-Efficient Rack-Scale Computing Systems. *IEEE Transactions on Computer-Aided Design of Integrated Circuits and Systems* 39, 3 (2019), 626–639.

[35] Zhe Zhang, Chuan Wu, and Zongpeng Li. 2021. Near-Optimal Topology-adaptive Parameter Synchronization in Distributed DNN Training. In *IEEE INFOCOM 2021-IEEE Conference on Computer Communications*. IEEE, 1–10.